Phuong *et al. J Wireless Com Network* (2022) 2022:34
https://doi.org/10.1186/s13638-022-02118-2

EURASIP Journal on Wireless Communications and Networking

RESEARCH Open Access

Combining precoding and equalization for interference cancellation in MU-MIMO systems with high density users

Nguyen Thu Phuong, Vu Van Son and Pham Thanh Hiep*

*Correspondence:
phamthanhhiep@gmail.com
Faculty of Radio-Electronics Engineering, Le Quy Don Technical University, Ha Noi, Vietnam

Abstract

In multiple users (MU) multiple input multiple output (MIMO) systems, the non-orthogonal multiple access (NOMA) method can provide multiple access. However, a spectrum efficiency of NOMA method is restricted because of remaining an interference signal of another user. A beamforming method can also be applied into MU-MIMO systems for implementation of multiple access without the interference with the other users; however, it is unavailable for a high density user environment in which multiple users locate close to each other. In order to further improve the spectrum efficiency, we propose a novel signal processing method which joints a precoding and an equalization. First, a precoding matrix is prepared for every user at base station, and we design an equalization which is orthogonal to the precoding matrix. Second, a set of linear weights is proposed to calculate at users for cancelling any interference signal. Therefore, signals for other users are eliminated according to the orthogonal feature and linear signal processing, and then, every user can receive its own signal without the interference signal. The proposed method is compared with the beamforming and NOMA methods in several scenarios, and the calculation result shows that our method outperforms other methods. Especially, our novel method works properly in the case of high density users.

Keywords: Equalization design orthogonal to precoding, Multiple users interference cancellation, Multiple input multiple output, Channel capacity, Zero-forcing beamforming algorithm

1 Introduction

1.1 Related works

In recent years, many advanced technologies for multiple input multiple output (MIMO) communication systems have been proposed. A byword is the beamforming technology, which has attracted increasing research interest recently. In order to exploit the full potential of MIMO system and its expansion, the massive MIMO system, many beamforming algorithms were developed. Several well-known beamforming methods which generate multiple beams to serve multiple users (MU) in MU-MIMO systems were proposed, e.g. Zero-Forcing (ZF) beamforming [1–3], minimum mean square error (MMSE) beamforming [4–6], dirty paper coding (DPC) [7, 8], singular value decomposition

(SVD) [9–11]. However, most algorithms have assumed that perfect channel state information (CSI) is available at both transceivers and responds insensitively to change of transmission environment and relative position between transceivers. To solve these issues, an intelligent beamforming scheme was suggested. The intelligent beamforming is achievable by deployment of artificial intelligence (AI) techniques to generate beams for every user. The machine learning-based beamforming design was first introduced for two-user MIMO system with interference channels by Hyung et al. [12]. The proposed machine learning structure takes transmit power and channel vectors as input and then recommends two users to choice between MRT and ZF as output. An intelligent recommendation method also was proposed to support users in big data environments [13, 14]. Recently, in [15], the deep learning-assisted detection method has been proposed for MU-MIMO systems. As addressed by the authors, the proposed detection method outperforms the maximum likelihood detection (MLD) in the case of channel impairments with low complexity. Compared to conventional beamforming methods, the deep learning and machine learning-based beamforming methods can improve the performance of system, especially in rapid alteration of transmission environment. However, the improvement of spectrum efficiency of these method has not yet met the demand of growth of wireless devices.

In order to further improve the performance of massive MIMO systems, a full-space spectrum-sharing strategy [16], a unified transmission strategy for TDD/FDD [17], and the hybrid beamforming as a combination of digital baseband and analog RF phase shifters [18, 19] were proposed. The hybrid beamforming method increases an efficiency of beamforming, and hence, the performance of MU systems is improved. However, beamforming algorithms depend on the number of antennas at a base station (BS) as well as the number of users, and they are inefficient when the number of users is much more than the number of antennas at the BS. In millimeter-wave wireless communication systems, BSs are densely distributed in order to cover a wide service area [6, 20, 21]. Microcell and macrocell cover a wide area, and their BSs are equipped with many antennas. However, the number of antennas at the BS of picocell and femtocell is insufficient to generate an individual beam for every user because of limited setting space and many users. Especially, when many users locate close to each other, i.e., high density user systems, multiple users are affected by a beam of the BS which is generated for another user. Therefore, because of overlap of beams, it is unavailable to serve every user without the interference with the other users.

The non-orthogonal multiple access (NOMA) is a widely used approach to deal with the problem of multiple nearby users by providing the multiple access based on power domain [22, 23]. The NOMA method allocates more transmit power for users of low channel gain and less transmit power for users of high channel gain. At the user of low channel gain, it detects its own signal while considering signals of other users as interference. Whereas, at the user of high channel gain, it applies the successive interference cancellation (SIC) following the principle of NOMA method to eliminate signals of other users, and then detect its own signal. As mentioned in [24, 25], the combination of NOMA and beamforming methods has been proved as an effective method to increase the spectral efficiency of system. However, the disadvantage of NOMA method is to maintain the interference at the user of low channel gain, it lets

a signal-to-interference-plus-noise ratio (SINR) be low, and hence, the performance of NOMA systems is deteriorated, even for the combination of NOMA and beamforming methods.

1.2 Scope and contributions

As mentioned above, many technologies have developed to combine with the beamforming method in order to improve the spectral efficiency of wireless systems. However, the interference signal is still remained, especially in high density user systems. One of main reasons can be explained as follows. The beamforming method is applied only to the transmitter site or the receiver site. Therefore, the interference signal cannot be completely cancelled because of lack of rigor. We suggest that a combination of precoding at the transmitter site and equalization at the receiver site with utilization of orthogonal feature can further improve the spectral efficiency of MU-MIMO systems, even for high density user systems.

Consequently, in this paper, we propose a novel signal processing method to improve the performance of system in case the number of antennas at the BS is lack for generating individual beam for every users without overlapping. Our proposal method takes advantage of orthogonality between precoding and equalization to completely cancel interference signals of other users and maintain high quality of service.

The contributions of this paper can be summarized as follows:

- A systematic approach is presented for designing an equalization which is orthogonal to precoding matrix for cancelling the interference signal.
- A novel linear signal processing approach is proposed in order to calculate weights for detecting the designed signal.
- The correlation coefficient of channel matrices of nearby users is derived and taken into consideration. The derived correlation coefficient can be used as a means to evaluate the performance of proposed method in several scenarios, especially for the case of multiple nearby users.
- Various calculation and simulation results have been carried out to compare the efficiency of the proposed method with other methods, such as the NOMA and beamforming methods.
- we discuss on ability of extension and application of proposed method to actual systems.

The rest of paper is organized as follows. We briefly overview the model of MU-MIMO systems in high density user environment in Sect. 2. Also in this section, the conventional beamforming and NOMA methods are explained. The novel signal processing method for interference cancellation in downlink MU-MIMO systems is proposed in Sect. 3. Section 4 presents simulation results and analysis. Finally, the conclusion is drawn in Sect. 5.

Notations: Regular and bold styles denote a scalar and a vector/matrix, respectively. $\mathbf{X}^{\mathrm{T}}$, $\mathbf{X}^{\mathcal{H}}$ and $\mathbf{X}^{-1}$, respectively, depict the transpose, Hermitian and pseudo-inverse operations of $\mathbf{X}$. Because a component-wise form is utilized for analyzing the proposed system performance, $\mathbf{X}(\mathrm{l})$ or $\mathbf{XY}(\mathrm{l})$ represents the l^{th} row of matrix $\mathbf{X}$ or the l^{th} row of matrix $\mathbf{Z} = XY$.

$\mathbb{C}^{m\times n}$ denotes a m rows, n columns independent and identically distributed (i.i.d.) complex Gaussian entries matrix which is normalized with zero mean unit variance. $\mathbb{E}\{\cdot\}$ denotes the average operator.

2 System model of MU-MIMO systems

2.1 MU-MIMO system model with high density users

Figure 1 shows a MU-MIMO communication system configuration which is equipped with a base station (BS) and K users. The number of antennas at the BS is denoted by M, whereas the number of antennas at every user is assumed to be two (2) due to limitation space of personal devices. In order to communicate with all users, the zero forcing beamforming (ZFBF) algorithm is applied at the BS due to its simplicity. Thanks to the beamforming method, the BS can communicate to each user via individual beams. However, despite the aforementioned advantage, this method suffers from overlap between beams when K users are in the same direction. This means that the MU-MIMO system still faces the problem of interference, which possibly degrades the system performance.

Under the assumptions that the channel response matrix between the BS and User i, $\mathbf{H}_i$, is block fading, and the entries of $\mathbf{H}_i$ are independent and identically distributed (i.i.d.) complex Gaussian random variables with zero mean and unit variance. Let $\mathbf{H}_i = \{h^i_{l,m}\} \in \Omega_i\mathbb{C}^{2\times M}$ with $i \in 1,\ldots,K$. $h^i_{l,m}$ represents the channel coefficient between the m^{th} antenna of BS and the l^{th} antenna of User i, and Ω_i denotes the variance of channel gain between the BS and User i. Without loss of generality, we assume that $\Omega_K > \cdots > \Omega_2 > \Omega_1$. In other words, the Users $K,\ldots,2,1$ are arranged farther away, the User 1 is the farthest user, whereas the User K is the nearest user.

Furthermore, the channel state information at transmitter (CSIT) is assumed to be outdated due to the delay of feedback transmission from users to the BS. The true and the error channel matrices of User i are, respectively, denoted by $\mathbf{H}^t_i$ and $\mathbf{H}^e_i$. Therefore, the estimated channel matrix $\mathbf{H}_i$ is calculated via a correlation coefficient of the estimated and true channel matrices, ρ, as follows [26, 27]:

$$\mathbf{H}_i = \sqrt{1-\rho^2}\mathbf{H}^e_i + \rho\mathbf{H}^t_i. \tag{1}$$

According to the ZFBF algorithm, the weight $\mathbf{w}_i$ for the User i is given by [23, 28]

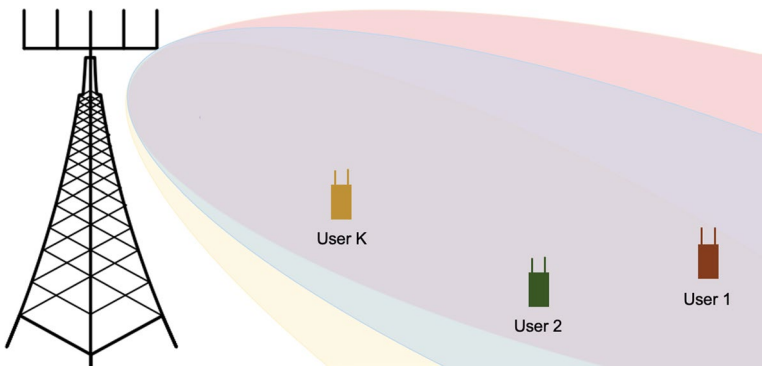

Fig. 1 System model of MU-MIMO systems consisting of K users in the same beam

$$\mathbf{w}_i = \frac{\mathbf{W}_i \mathbf{H}_i}{\|\mathbf{W}_i \mathbf{H}_i\|}, \tag{2}$$

where

$\mathbf{W}_i = \mathbf{I} - \mathbb{H}_i(\mathbb{H}_i^H \mathbb{H}_i)^{-1}\mathbb{H}_i^H$,
$\mathbb{H}_i = [\mathbf{H}_1, \mathbf{H}_2, \ldots, \mathbf{H}_{i-1}, \mathbf{H}_{i+1}, \ldots, \mathbf{H}_K]$,
and $\mathbf{I}$ is an identity matrix.

The weight $\mathbf{w}_i$ ensures that the BS can communicate with the User i via its own beam, and the interference with other users can be avoided if the beam is sharp enough or the user is far from each other. However, the number of antennas at the BS is not enough to generate a sharp beam and many users are close to each other in high density user environment. Therefore, the interference signal is still remained and depends on an overlap factor of beams.

2.2 Conventional beamforming and NOMA methods

2.2.1 Beamforming method

In the system utilizing beamforming method, the BS applies the ZFBF method, and the weight is generated by (2). Firstly, information signals of all users are multiplied by their own weight and transmitted via the transmit antenna of BS [23, 28].

$$\mathbf{X}^{\text{BEAM}} = \sum_{k=1}^{K} \mathbf{w}_k \sqrt{a_k \text{p}} \mathbf{S}_k, \tag{3}$$

where p denotes the transmit power of BS, a_k is the power allocation coefficient of the User k, and $\mathbf{S}_k = [s_{\text{k1}}, s_{\text{k2}}]^{\text{T}}$ represents the information signal of User k. In order to provide the same quality of service (QoS) for every user, we assume that a_k is inversely proportional to the channel gain and subject to $\sum_{k=1}^{K} a_k = 1$. The power allocation coefficient is proposed to calculate by

$$a_k = \frac{\sum_{i,j=1}^{K} \prod^{i,j\neq k} \Omega_i \Omega_j}{\sum_{i,j=1}^{K} \prod \Omega_i \Omega_j}. \tag{4}$$

In spite of application of ZFBF method, the received signal at the User i still includes the signal of others because of overlap of beams.

$$\begin{aligned} \mathbf{Y}_i^{\text{BEAM}} &= \mathbf{H}_i \mathbf{X}^{\text{BEAM}} + \mathbf{n}_i \\ &= \mathbf{H}_i \sum_{k=1}^{K} \mathbf{w}_k \sqrt{a_k \text{p}} \mathbf{S}_k + \mathbf{n}_i \\ &= \underbrace{\mathbf{H}_i \mathbf{w}_i \sqrt{a_i \text{p}} \mathbf{S}_i}_{\text{Desired signal of User } i} + \underbrace{\mathbf{H}_i \sum_{k=1,\neq i}^{K} \mathbf{w}_k \sqrt{a_k \text{p}} \mathbf{S}_k}_{\text{Interference signals}} + \mathbf{n}_i, \end{aligned} \tag{5}$$

where $\mathbf{n}_i \in \sigma_i^2 \mathbb{C}^{2\times 1}$ denotes the thermal noise vector at the User i, and σ_i^2 represents the variance of noise vector. We assumed that the variance of noise vector for all users is the same, $\sigma_1^2 = \sigma_2^2 = \cdots = \sigma_K^2 = \sigma^2$.

As defined in (2), the weight depends on the channel response matrix and $\mathbf{H}_i\mathbf{w}_k = \mathbf{0}$ ($i \neq k$), $\mathbf{H}_i\mathbf{w}_i = \mathbf{I}$ in case the users are far from each other. However, in this work, we assumed that the users are close to each other. Therefore, γ_{ik}, $0 \leq \gamma_{ik} \leq 1$, is defined as the overlap factor of beams of Users i and k. $\gamma_{ik} = 1$ means that the User i locates on the center line of the beam for the User k. The γ_{ik} decreases when they move forward to the edge of the other's beam, and $\gamma_{ik} = 0$ when they are located out site of the other's beam. Moreover, the CSIT is outdated, and then, the first term in (5) is represented by

$$\mathbb{E}\{\mathbf{H}_i\mathbf{w}_i\sqrt{a_i \mathrm{p}}\mathbf{S}_i\} = \rho^2\Omega_i a_i \mathrm{p} + (1-\rho^2)\Omega_i a_i \mathrm{p}. \tag{6}$$

In the right side of (6), the first term is the useful one which is used to detect the designed signal, whereas the second term is the interference one which is established due to the estimation error of channel matrix. The interference term in (5) is depicted as

$$\mathbb{E}\{\mathbf{H}_i \sum_{k=1,\neq i}^{K} \mathbf{w}_k\sqrt{a_k \mathrm{p}}\mathbf{S}_k\} = \sum_{k=1,\neq i}^{K} \left((1-\rho^2) + \gamma_{ik}\rho^2\right)\Omega_i a_k \mathrm{p}. \tag{7}$$

The term of $(1-\rho^2)$ is due to channel estimation error, and the term of $\gamma_{ik}\rho^2$ is due to the overlap of beams of Users i and k.

As a result, the signal-to-interference-plus-noise ratio (SINR) of User i is depicted as

$$\begin{aligned} \mathrm{SINR}_i^{\mathrm{BEAM}} &= \frac{\rho^2\Omega_i a_i \mathrm{p}}{(1-\rho^2)\Omega_i a_i \mathrm{p} + \sum_{k=1,\neq i}^{K}\left(1-\rho^2+\gamma_{ik}\rho^2\right)\Omega_i a_k \mathrm{p} + \sigma^2} \\ &= \frac{\rho^2\Omega_i a_i \delta}{(1-\rho^2)\Omega_i a_i \delta + \sum_{k=1,\neq i}^{K}\left(1-\rho^2+\gamma_{ik}\rho^2\right)\Omega_i a_k \delta + 1}, \end{aligned} \tag{8}$$

where $\delta = \frac{\mathrm{p}}{\sigma^2}$.

2.2.2 NOMA method

In the system utilizing NOMA methods, the BS provides multiple access base on power domain. The higher transmit power is allocated for the user of low channel gain, and the lower transmit power is allocated for the user of high channel gain. We assume that the power correlation coefficient in (4) is applied into the NOMA system. The BS simultaneously broadcasts information signals to K users with different power levers [23, 24].

$$\mathbf{X}^{\mathrm{NOMA}} = \sum_{k=1}^{K} \sqrt{a_k \mathrm{p}}\mathbf{S}_k. \tag{9}$$

The user i receives the information signal of all users [23, 24].

$$\begin{aligned}\mathbf{Y}_i^{\text{NOMA}} &= \mathbf{H}_i \sum_{k=1}^{K} \sqrt{a_k \text{p}} \mathbf{S}_k + \mathbf{n}_i \\ &= \underbrace{\mathbf{H}_i \sqrt{a_i \text{p}} \mathbf{S}_i}_{\text{Desired signal of User } i} + \underbrace{\mathbf{H}_i \sum_{k=1,\neq i}^{K} \sqrt{a_k \text{p}} \mathbf{S}_k}_{\text{Interference signals}} + \mathbf{n}_i. \end{aligned} \tag{10}$$

According to the principle of NOMA, the power allocation coefficient is inversely proportional to the channel gain, i.e., $a_1 > a_2 > \cdots > a_K$, and hence, the User i firstly utilizes the SIC operation to cancel the signal of users 1, 2, $\cdots$, $i-1$ and then detects its own signal while considering the signal of users $i+1$, $\cdots$, K as interference. However, because of the outdated CSIT, the interference from users 1, 2, $\cdots$, $i-1$ is incompletely cancelled. Therefore, the SINR of User i is represented as

$$\text{SINR}_i^{\text{NOMA}} = \frac{\rho^2 a_i \Omega_i \delta}{\sum_{k=1}^{i-1} (1-\rho^2) a_k \Omega_i \delta + \sum_{k=i+1}^{K} a_k \Omega_i \delta + 1} \tag{11}$$

3 Proposal of novel signal processing method

In order to cancel the interference signal, we propose the novel signal processing method which combines the precoding and equalization, furthermore, utilizes a linear signal processing at the user site. Our method can extract the desired signal of every user without the interference signal. However, the CSIT is assumed to be outdated, and the residual interference at the user in the proposed system should be investigated. The detail of proposed method for the desired User i while considering the signal for other users as the interference signal is explained below.

3.1 The structure of proposed method

The proposed signal processing method is illustrated in Fig. 2, and information signals of all users firstly are multiplied by the prepared precoding matrix, $\mathbf{P}_k$, and then broadcast. Hence, the transmit signal at the transmit antenna of BS is represented by

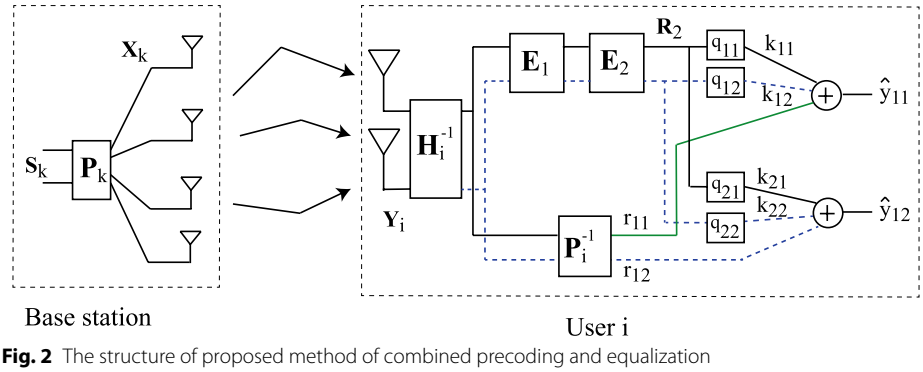

Fig. 2 The structure of proposed method of combined precoding and equalization

$$\mathbf{X} = \sum_{k=1}^{K} \mathbf{X}_k = \sum_{k=1}^{K} \mathbf{P}_k \sqrt{a_k \mathrm{p}} \mathbf{S}_k, \tag{12}$$

and, the received signal of User i is depicted as

$$\begin{aligned} \mathbf{Y}_i &= \mathbf{H}_i \sum_{k=1}^{K} \mathbf{P}_k \sqrt{a_k \mathrm{p}} \mathbf{S}_k + \mathbf{n}_i, \\ &= \underbrace{\mathbf{H}_i \mathbf{P}_i \sqrt{a_i \mathrm{p}} \mathbf{S}_i}_{\text{Desired signal of User } i} + \underbrace{\mathbf{H}_i \sum_{k=1, \neq i}^{K} \mathbf{P}_k \sqrt{a_k \mathrm{p}} \mathbf{S}_k}_{\text{Interference signals}} + \mathbf{n}_i, \end{aligned} \tag{13}$$

Without loss of generality, we are going to explain the proposed method at the User i while considering the signal of other users as the interference signal.

3.2 Designing equalization orthogonal to precoding

As shown in Fig. 2, after being multiplied by $\mathbf{H}_i^{-1}$ to cancel the effect of propagation channel, the received signal of User i in (13) is processed parallelly to cancel the signal of the others. In the first stream, the received signal is multiplied by $\mathbf{P}_{\mathrm{i}}^{-1}$ to eliminate the precoding process, and we have

$$\begin{aligned} \mathbf{R}_1 &\equiv \begin{bmatrix} \mathrm{r}_{11} \\ \mathrm{r}_{12} \end{bmatrix} = (\mathbf{H}_i \mathbf{P}_i)^{-1} \mathbf{Y}_i, \\ &= \Omega_i \sqrt{a_i \mathrm{p}} \mathbf{S}_i + \Omega_i \mathbf{P}_i^{-1} \sum_{k=1, \neq i}^{K} \mathbf{P}_k \sqrt{a_k \mathrm{p}} \mathbf{S}_k + (\mathbf{H}_i \mathbf{P}_i)^{-1} \mathbf{n}_i. \end{aligned} \tag{14}$$

The term of $\sum_{k=1, \neq i}^{K} \mathbf{P}_k \sqrt{a_k \mathrm{p}} \mathbf{S}_k$ represents by an 2×1 vector, and hence, we can rewrite it in another form which includes an amplification factor Γ, and a vector $\tilde{\mathbf{S}} = [\tilde{s}_1 \ \ \tilde{s}_2]^T \in \mathbb{C}^{2\times 1}$.

$$\Gamma \tilde{\mathbf{S}} \equiv \sum_{k=1, \neq i}^{K} \mathbf{P}_k \sqrt{a_k \mathrm{p}} \mathbf{S}_k. \tag{15}$$

To notice that $\mathbb{E}\{ \sum_{k=1, \neq i}^{K} \mathbf{P}_k \sqrt{a_k \mathrm{p}} \mathbf{S}_k \} = \sum_{k=1, \neq i}^{K} a_k \mathrm{p}$. Consequently, Eq. (14) is rewritten as

$$\mathbf{R}_1 = \Omega_i \sqrt{a_i \mathrm{p}} \mathbf{S}_i + \Omega_i \mathbf{P}_i^{-1} \Gamma \tilde{\mathbf{S}} + (\mathbf{H}_i \mathbf{P}_i)^{-1} \mathbf{n}_i. \tag{16}$$

As shown in (13), the second term is the interference signal that should be eliminated. In order to cancel the interference signal, in the second stream, the received signal is multiplied by two equalization matrices, $\mathbf{E}_1 \in \mathbb{C}^{2\times 2}$ and $\mathbf{E}_2 \in \mathbb{C}^{2\times 2}$, which are designed to be orthogonal to the precoding matrix of User i, i.e. $\mathbf{E}_2 \mathbf{E}_1 \mathbf{P}_i = 0$.

The detail of designing these two equalization matrices is explained as follows. Let

$$\mathbf{P}_i = \begin{bmatrix} \mathrm{p}_{11} & \mathrm{p}_{12} \\ \mathrm{p}_{21} & \mathrm{p}_{22} \end{bmatrix}. \tag{17}$$

To create the matrix $\mathbf{E}_1$ subject to

$$\begin{aligned} \mathbf{E}_1(1) \begin{bmatrix} \mathrm{p}_{11} \\ \mathrm{p}_{21} \end{bmatrix} &= 0, \\ \mathbf{E}_1(2) \begin{bmatrix} \mathrm{p}_{11} \\ \mathrm{p}_{21} \end{bmatrix} &= 0. \end{aligned} \tag{18}$$

Consequently,

$$\mathbf{E}_1 \mathbf{P}_i = \begin{bmatrix} 0 & \hat{p}_{12} \\ 0 & \hat{p}_{22} \end{bmatrix}. \tag{19}$$

And then, to create $\mathbf{E}_2$ subject to

$$\begin{aligned} \mathbf{E}_2(1) \begin{bmatrix} \hat{p}_{12} \\ \hat{p}_{22} \end{bmatrix} &= 0, \\ \mathbf{E}_2(2) \begin{bmatrix} \hat{p}_{12} \\ \hat{p}_{22} \end{bmatrix} &= 0. \end{aligned} \tag{20}$$

An example of the matrices is presented by

$$\begin{aligned} \mathbf{E}_1 &\equiv \frac{1}{\sqrt{p_{21}^2 + \mathrm{p}_{11}^2}} \begin{bmatrix} -\mathrm{p}_{21} & \mathrm{p}_{11} \\ -\mathrm{p}_{21} & \mathrm{p}_{11} \end{bmatrix}. \\ \mathbf{E}_2 &\equiv \frac{1}{\sqrt{2}} \begin{bmatrix} -1 & 1 \\ -1 & 1 \end{bmatrix}. \end{aligned} \tag{21}$$

Since the matrix $\mathbf{E} = \mathbf{E}_2\mathbf{E}_1$ is orthogonal to $\mathbf{P}_i$, we have

$$\begin{aligned} \mathbf{R}_2 \equiv & \mathbf{E}_2\mathbf{E}_1\mathbf{H}_i^{-1}\mathbf{Y}_i, \\ = & \mathbf{E}_2\mathbf{E}_1\mathbf{H}_i^{-1}\left(\mathbf{H}_i\mathbf{P}_i\sqrt{a_i}\mathrm{p}\mathbf{S}_i + \mathbf{H}_i\sum_{k=1,\neq i}^{K}\mathbf{P}_k\sqrt{a_k}\mathrm{p}\mathbf{S}_k + \mathbf{n}_i\right), \\ = & \mathbf{E}_2\mathbf{E}_1\left(\mathbf{P}_i\Omega_i\sqrt{a_i}\mathrm{p}\mathbf{S}_i + \Omega_i\Gamma\tilde{\mathbf{S}} + \mathbf{H}_i^{-1}\mathbf{n}_i\right), \\ = & \mathbf{E}_2\mathbf{E}_1\Omega_i\Gamma\tilde{\mathbf{S}} + \mathbf{E}_2E_1\mathbf{H}_i^{-1}\mathbf{n}_i, \\ = & \mathbf{E}\Omega_i\Gamma\tilde{\mathbf{S}} + \tilde{\mathbf{n}}, \end{aligned} \tag{22}$$

where $\tilde{\mathbf{n}} = \mathbf{E}_2E_1\mathbf{H}_i^{-1}\mathbf{n}_i$.

3.3 Linear signal processing for interference cancellation

After that, the $\mathbf{R}_2$ signal is controlled linearly by four weights, $q_{ij},\ i,j \in \{1,2\}$, as shown in Fig. 2.

$$k_{11} = q_{11}\mathbf{R}_2(1), \;\; k_{12} = q_{12}\mathbf{R}_2(2),$$
$$k_{21} = q_{21}\mathbf{R}_2(1), \;\; k_{22} = q_{22}\mathbf{R}_2(2).$$

Therefore, we have

$$\begin{aligned}\hat{y}_{11} \equiv & r_{11} + k_{11} + k_{12},\\ = & \mathbf{R}_1(1) + q_{11}\mathbf{R}_2(1) + q_{12}\mathbf{R}_2(2),\\ = & \{\Omega_i\sqrt{a_i \mathrm{p}}\mathbf{S}_i + \Omega_i\mathbf{P}_i^{-1}\Gamma\tilde{\mathbf{S}} + (\mathbf{H}_i\mathbf{P}_i)^{-1}\mathbf{n}_i\}(1)\\ & + q_{11}\{\mathbf{E}\Omega_i\Gamma\tilde{\mathbf{S}} + \tilde{\mathbf{n}}\}(1) + q_{12}\{\mathbf{E}\Omega_i\Gamma\tilde{\mathbf{S}} + \tilde{\mathbf{n}}\}(2),\\ = & \Omega_i\sqrt{a_i \mathrm{p}}\mathbf{S}_i(1) + \Omega_i\Gamma\left(\mathbf{P}_i^{-1}\tilde{\mathbf{S}}(1) + q_{11}\mathbf{E}\tilde{\mathbf{S}}(1) + q_{12}\mathbf{E}\tilde{\mathbf{S}}(2)\right)\\ & + (\mathbf{H}_i\mathbf{P}_i)^{-1}\mathbf{n}_i(1) + q_{11}\tilde{\mathbf{n}}(1) + q_{12}\tilde{\mathbf{n}}(2)\end{aligned} \tag{23}$$

The term of $\Omega_i\sqrt{a_i \mathrm{p}}\mathbf{S}_i(1)$ is the designed signal which should be detected, the term of $(\mathbf{H}_i\mathbf{P}_i)^{-1}\mathbf{n}_i(1) + q_{11}\tilde{\mathbf{n}}(1) + q_{12}\tilde{\mathbf{n}}(2)$ is the noise, and the remained term in the right site of (23) is the interference signal. It is completely removed when the linear weights q_{11} and q_{12} satisfy with following condition for any $\tilde{\mathbf{S}}$.

$$\Omega_i\Gamma\left(\mathbf{P}_i^{-1}\tilde{\mathbf{S}}(1) + q_{11}\mathbf{E}\tilde{\mathbf{S}}(1) + q_{12}\mathbf{E}\tilde{\mathbf{S}}(2)\right) = 0. \tag{24}$$

Detailing (24), the metric can be expressed as

$$\begin{bmatrix}\tilde{p}_{11}\tilde{p}_{12}\\ \tilde{p}_{21}\tilde{p}_{22}\end{bmatrix}\begin{bmatrix}\tilde{s}_1\\ \tilde{s}_2\end{bmatrix}(1) + q_{11}\begin{bmatrix}E_{11}E_{12}\\ E_{21}E_{22}\end{bmatrix}\begin{bmatrix}\tilde{s}_1\\ \tilde{s}_2\end{bmatrix}(1) + \mathrm{q}_{12}\begin{bmatrix}E_{11}E_{12}\\ E_{21}E_{22}\end{bmatrix}\begin{bmatrix}\tilde{s}_1\\ \tilde{s}_2\end{bmatrix}(2) = 0, \tag{25}$$

where $\mathbf{P}_i^{-1} \equiv \begin{bmatrix}\tilde{p}_{11} & \tilde{p}_{12}\\ \tilde{p}_{21} & \tilde{p}_{22}\end{bmatrix}$ and $\mathbf{E} \equiv \begin{bmatrix}E_{11}E_{12}\\ E_{21}E_{22}\end{bmatrix}$. After some manipulations, we have

$$(\tilde{p}_{11}+q_{11}E_{11}+q_{12}E_{21})\tilde{s}_1 + (\tilde{p}_{12}+q_{11}E_{12}+q_{12}E_{22})\tilde{s}_2 = 0. \tag{26}$$

Because the above equation should be satisfied for all $\tilde{s}_1$ and $\tilde{s}_2$, it is separated into two equations.

$$\begin{aligned}\tilde{p}_{11} + q_{11}E_{11} + q_{12}E_{21} = & 0,\\ \tilde{p}_{12} + q_{11}E_{12} + q_{12}E_{22} = & 0.\end{aligned} \tag{27}$$

Consequently,

$$\begin{aligned}q_{11} = & \frac{\tilde{p}_{12}E_{21} - \tilde{p}_{11}E_{22}}{E_{11}E_{22} - E_{12}E_{21}},\\ q_{12} = & \frac{\tilde{p}_{12}E_{11} - \tilde{p}_{11}E_{12}}{E_{21}E_{12} - E_{22}E_{11}}.\end{aligned} \tag{28}$$

From (23)and (24), we have the first signal of User i without the interference signal.

$$\hat{y}_{11} = \Omega_i\sqrt{a_i \mathrm{p}}s_{11} + (\mathbf{H}_i\mathbf{P}_i)^{-1}\mathbf{n}_i(1) + q_{11}\tilde{\mathbf{n}}(1) + q_{12}\tilde{\mathbf{n}}(2). \tag{29}$$

Similar to calculation of $\hat{y}_{11}$, the $\hat{y}_{12}$ is represented by

$$\begin{aligned}\hat{y}_{12} \equiv & r_{12} + k_{21} + k_{22},\\ =& \mathbf{R}_1(2) + q_{21}\mathbf{R}_2(1) + q_{22}\mathbf{R}_2(2),\\ =& \{\Omega_i\sqrt{a_i \mathrm{p}}\mathbf{S}_i + \Omega_i\mathbf{P}_i^{-1}\Gamma\tilde{\mathbf{S}} + (\mathbf{H}_i\mathbf{P}_i)^{-1}\mathbf{n}_i\}(2)\\ &+ q_{21}\{\mathbf{E}\Omega_i\Gamma\tilde{\mathbf{S}} + \tilde{\mathbf{n}}\}(1) + q_{22}\{\mathbf{E}\Omega_i\Gamma\tilde{\mathbf{S}} + \tilde{\mathbf{n}}\}(2),\\ =& \Omega_i\sqrt{a_i \mathrm{p}}\mathbf{S}_i(2) + \Omega_i\Gamma\left(\mathbf{P}_i^{-1}\tilde{\mathbf{S}}(2) + q_{21}\mathbf{E}\tilde{\mathbf{S}}(1) + q_{22}\mathbf{E}\tilde{\mathbf{S}}(2)\right)\\ &+ (\mathbf{H}_i\mathbf{P}_i)^{-1}\mathbf{n}_i(2) + q_{21}\tilde{\mathbf{n}}(1) + q_{22}\tilde{\mathbf{n}}(2).\end{aligned} \tag{30}$$

Therefore, the $\hat{y}_{12}$ can be obtained without the interference signal under the following condition.

$$\mathbf{P}_i^{-1}\tilde{\mathbf{S}}(2) + q_{21}\mathbf{E}\tilde{\mathbf{S}}(1) + q_{22}\mathbf{E}\tilde{\mathbf{S}}(2) = 0. \tag{31}$$

The noise component is assumed to be uncorrelated with the other, by applying the average operation for the received signal in (29), and the SNR of User i is described by

$$\mathrm{SNR}_i = \frac{\mathbb{E}\{\Omega_i\sqrt{a_i \mathrm{p}}s_{11}\}}{\mathbb{E}\{(\mathbf{H}_i\mathbf{P}_i)^{-1}\mathbf{n}_i(1) + q_{11}\tilde{\mathbf{n}}(1) + q_{12}\tilde{\mathbf{n}}(2)\}} = \frac{\Omega_i^2 a_i \mathrm{p}}{\sigma^2(1 + \mathrm{q}_{11}^2 + \mathrm{q}_{12}^2)}. \tag{32}$$

However, in the case of outdate CSIT, the $\mathbf{R}_1$ in (16) still has the inseparable term, $(1-\rho^2)\Omega_i\sqrt{a_i \mathrm{p}}\mathbf{S}_i$, and it becomes an interference signal. Similarly, in $\mathbf{R}_2$ of (22), $\mathbf{P}_i\Omega_i\sqrt{a_i \mathrm{p}}\mathbf{S}_i$ is not clearly cancelled by the condition of $\mathbf{E}_2\mathbf{E}_1\mathbf{P}_i = 0$, and hence, the term of $(1-\rho^2)\mathbf{P}_i\Omega_i\sqrt{a_i \mathrm{p}}\mathbf{S}_i$ is still remained. Moreover, $\Omega_i\mathbf{P}_i^{-1}\Gamma\tilde{\mathbf{S}}$ of $\mathbf{R}_1$ and $\mathbf{E}\Omega_i\Gamma\tilde{\mathbf{S}}$ of $\mathbf{R}_2$ are not removed completely, apart of them, i.e., $(1-\rho^2)\Omega_i\mathbf{P}_i^{-1}\Gamma\tilde{\mathbf{S}}$ and $(1-\rho^2)\mathbf{E}\Omega_i\Gamma\tilde{\mathbf{S}}$, is added into the received signal as interference. Consequently, the total of interference signal due to the outdated CSIT is represented as $(1-\rho^2)\Omega_i\sqrt{a_i \mathrm{p}}(\mathbf{I} + \mathbf{P}_i)\mathbf{S}_i + (1-\rho^2)\Omega_i\Gamma(\mathbf{P}_i^{-1} + \mathbf{E})\tilde{\mathbf{S}}$.

As a result, the SINR of User i in the case of outdated CSIT is represented by

$$\begin{aligned}\mathrm{SINR}_i &= \frac{\rho^4\Omega_i^2 a_i \mathrm{p}}{2(1-\rho^2)^2\Omega_i^2 a_i \mathrm{p} + 2(1-\rho^2)^2\Omega_i^2\sum\limits_{k=1,\neq i}^{K} a_k \mathrm{p} + (1 + q_{11}^2 + q_{12}^2)\sigma^2},\\ &= \frac{\rho^4\Omega_i^2 a_i \mathrm{p}}{2(1-\rho^2)^2\Omega_i^2\sum\limits_{k=1}^{K} a_k \mathrm{p} + (1 + q_{11}^2 + q_{12}^2)\sigma^2},\\ &= \frac{\rho^4\Omega_i^2 a_i \mathrm{p}}{2(1-\rho^2)^2\Omega_i^2 \mathrm{p} + (1 + q_{11}^2 + q_{12}^2)\sigma^2}.\end{aligned} \tag{33}$$

Moreover, from the (24), we have

$$\mathbb{E}\{q_{11}\mathbf{E}_1\mathbf{S}_2(1) + q_{12}\mathbf{E}_1\mathbf{S}_2(2)\} = \mathbb{E}\{\mathbf{P}_1^{-1}\mathbf{P}_2\mathbf{S}_2(2)\}. \tag{34}$$

To notice that all matrices are normalized, the component of information signal is uncorrelated with the other, and hence

$$q_{11}^2 + q_{12}^2 = 1. \tag{35}$$

Thus, the SINR in (33) is rewritten as

$$\begin{aligned}\mathrm{SINR}_i &= \frac{\rho^4\Omega_i^2 a_i \mathrm{p}}{2(1-\rho^2)^2\Omega_i^2\mathrm{p}+2\sigma^2},\\ &= \frac{\rho^4\Omega_i^2 a_i \delta}{2(1-\rho^2)^2\Omega_i^2\delta+2}.\end{aligned} \tag{36}$$

The channel capacity of users is calculated by the Shannon theory.

$$C_i = \log_2(1+\mathrm{SINR}_i) \ \ [\mathrm{bit/s/Hz}]. \tag{37}$$

4 Calculation results and discussion

In this section, we investigate the performance of proposed method via channel capacity based on several parameters and compare to the NOMA and beamforming methods. Their channel capacity is calculated by (37), whereas the SINR of beamforming, NOMA and proposed methods is, respectively, calculated by (8), (11) and (36). For simplicity, we assume that the factors ρ and γ_{ij} are the same for all users, $\gamma_{ij} = \gamma$ for all i, j. The parameters of system are changed in turn in order to investigate their impact on the performance of system while fixing the other parameters. The initial parameters are set as follows: $K = 4, \Omega_K = 0$ dB, $\Omega_k = \Omega_{k+1} - 1$ for $k \in \{1, \ldots, K-1\}$, $\rho = 0.8$, $\gamma = 0.9$.

4.1 Comparison of channel capacity based on δ

The channel capacity of all methods via δ with above mentioned parameters is represented in Fig. 3. The channel capacity is increased when the δ increases; however, it is saturated with high δ. The reason is that when the δ increases, the designed signal power is increased; however, the interference signal power is also increased. Therefore,

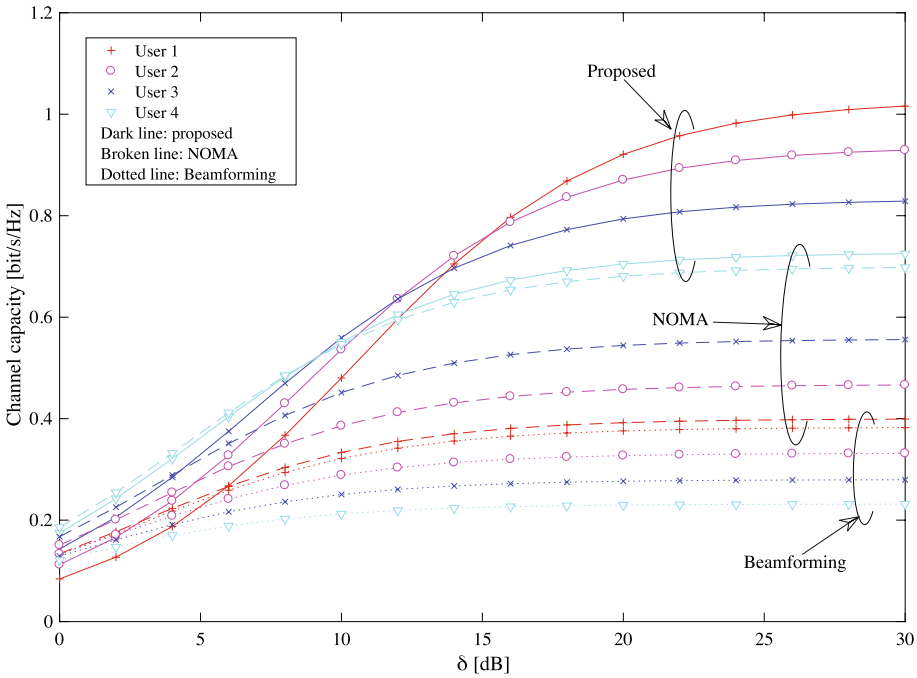

Fig. 3 The channel capacity via the number of users in the case of $\Omega_K = 0$ dB, $K = 4$

the SINR and the channel capacity become saturated. Compared with the NOMA and beamforming methods, the proposed method outperforms, especially in high δ regime. It confirms the advantage of our novel method that can remove the interference signal by the orthogonal feature and the linear signal processing.

For the proposed method, in low δ regime, the received signal of farther users is weak; hence, their channel capacity is low. However, in high δ regime, the designed signal of farther users and the interference signal of nearer users are increased. Consequently, the SINR of farther users is improved considerably, whereas that of nearer users is improved slowly following the increase in δ. It is the reason why the channel capacity of User 1 increases rapidly and be the highest from 15 dB of the δ. The beamforming method is similar, the far user has the higher transmit power, and it interferes with the near user due to the overlap of beamforming. In contrast to both above methods, in the case of NOMA method, the User 1 detects its own signal while considering the signal of other users as interference. Whereas, the nearer user detects its own signal by applying SIC operation to remove the signal of other users. However, the SIC operation is imperfect because of the outdated CSIT. Therefore, the signal of other users is still remained as interference. To compare to the remaining interference caused by imperfect SIC operation, the power of nearer user signal is higher, and hence, the SINR of nearer user is higher.

4.2 Comparison of channel capacity based on *K*

The investigation of channel capacity with $K = 8$ is shown in Fig. 4 which includes the channel capacity of Users 2, 4, 6 and 8 of three methods. The system model is similar to the model of Fig. 3, and the result is also similar. However, the saturation value is different from the case of $K = 4$. The reason is that the transmit power of every user is changed according to the number of users. Furthermore, the interference signal in the

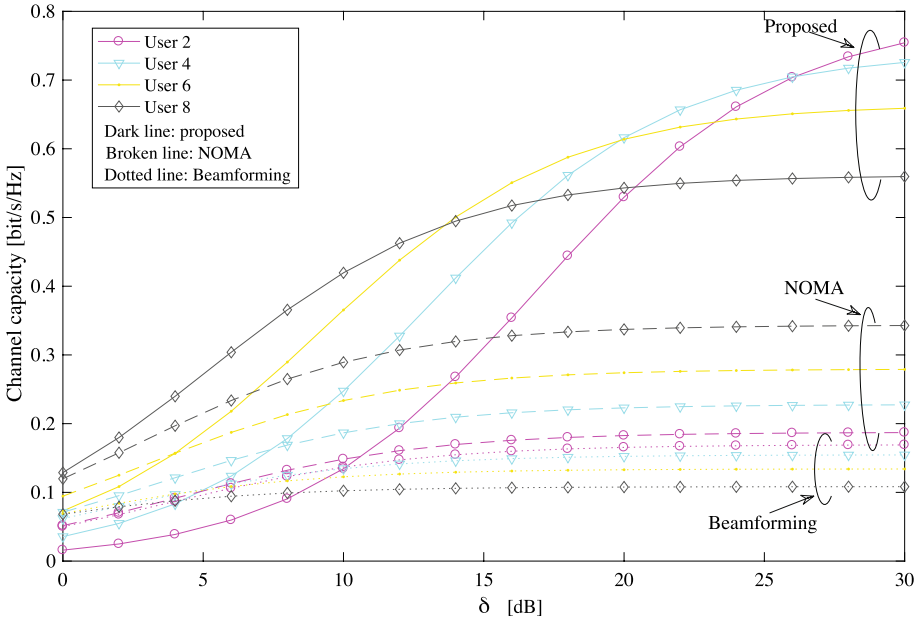

Fig. 4 The channel capacity via the number of users in the case of $\Omega_K = 0$ dB, $K = 8$

case of $K = 8$ should include the signal of 7 other users. Therefore, the SINR and the channel capacity in this case are lower.

4.3 Channel capacity of all methods under different channel gain

Figures 5 and 6 illustrate the channel capacity of all methods in the case of $\Omega_K = 5\,\text{dB}$ and -5 dB, respectively. The increase in Ω_K variance means that the channel gain is improved. Therefore, the channel capacity of high Ω_K is higher; however, its saturation value is the same when the δ is high enough. From the above figures, we can recognize the impact of Ω_K on the performance of system. Our proposed method is sensitive to the channel gain, and it outperforms the NOMA and beamforming methods when the channel gain and/or the δ are high. However, its channel capacity is rapidly decreased when the channel gain and the δ become small.

4.4 The impact of overlap factor on the channel capacity

We investigate the impact of γ on the channel capacity at $\delta = 15\,\text{dB}$, and the result is shown in Fig. 7. The change of γ affects the performance of only beamforming method. Therefore, the channel capacity of 2 other methods is constant. The reduction of γ means that the overlap of beams is mitigated. Consequently, the interference between users is extenuated, and the channel capacity is improved. As expected, the channel capacity of beamforming method is considerably improved when the γ reduces, and it becomes the highest with $\gamma = 0$. In this scenario, the overlap of beams is absent, and every user is communicated by its individual beam. However, the inseparable term is still remained because of outdated CSIT, and it is considered as interference and lets the SINR of conventional beamforming method down. As a result, the channel capacity of beamforming

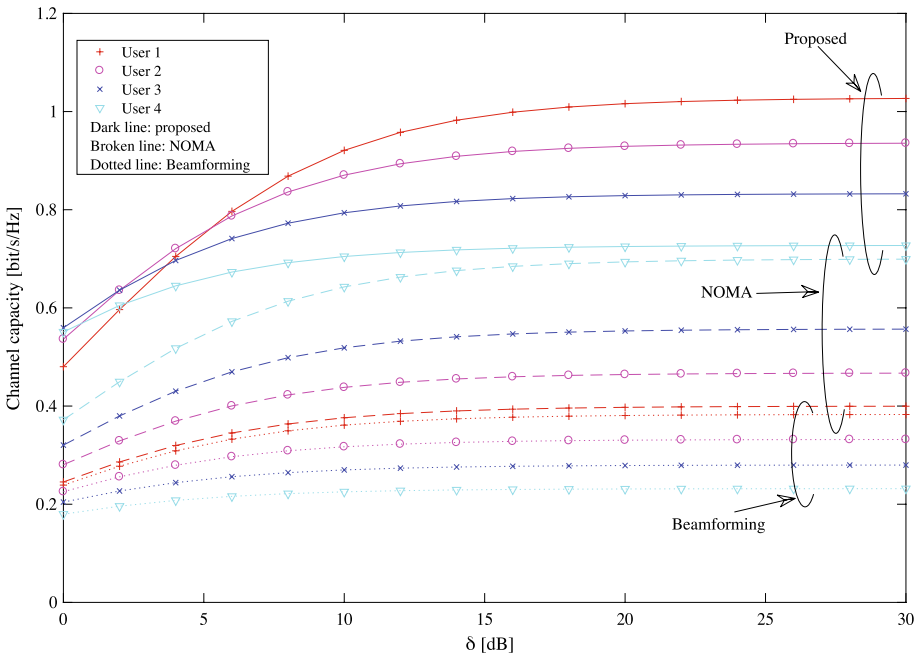

Fig. 5 The change of channel capacity according to $\Omega_K = 5$ dB

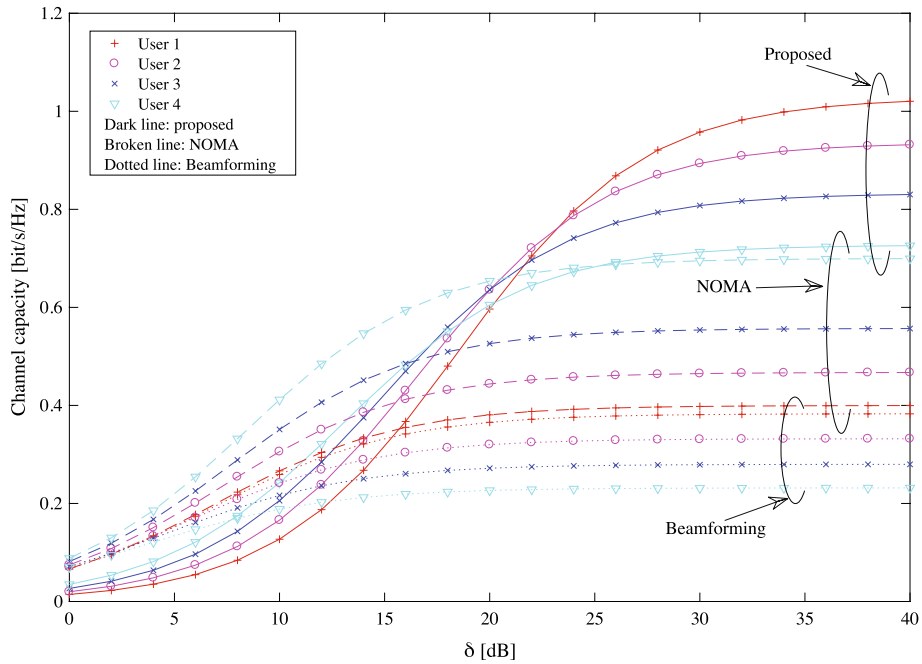

Fig. 6 The change of channel capacity according to $\Omega_K = -5$ dB

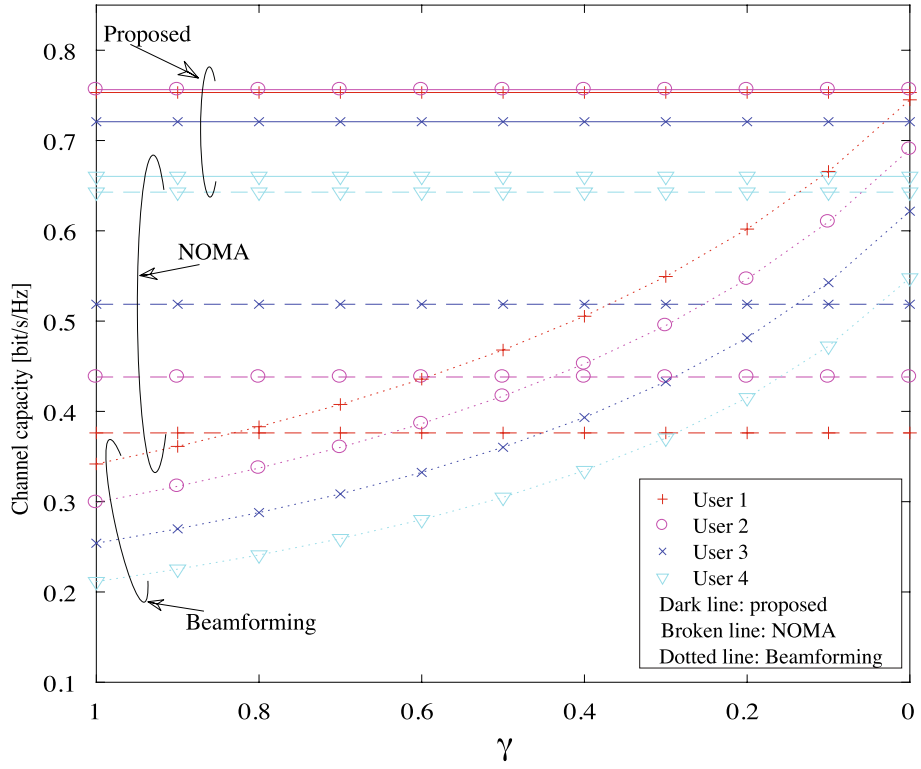

Fig. 7 The channel capacity via γ with $\delta = 15$ dB, $\rho = 0.8, K = 4$

method is lower than that of proposed method even in the case of $\gamma = 0$. It confirms the advantage of our novel method.

4.5 The effect of outdated CSIT

The effect of factor ρ on the channel capacity of considered methods is depicted in Figs. 8 and 9 with $\gamma = 0.2$ and 0.9, respectively. To notice that the factor ρ indicates the accuracy of estimated channel matrix comparing with the true one. From these figures we can say that, to estimate the channel matrix accurately is important, the channel capacity is considerably increased following the increase in factor ρ. Besides, the reduction of γ lets the channel capacity of beamforming method be improved as explained above. However, the channel capacity of 3 methods is low and almost the same for $\rho \leq 0.8$. For $\rho > 0.8$, the channel capacity of our novel method is increased more rapidly and becomes the highest one in both cases of γ.

5 Conclusion and future works

In this work, the novel method is proposed for cancelling the interference of MU-MIMO systems with high density users, and the proposed system is investigated in the case of multiple users and outdated CSIT. The outdated CSIT lets the interference cancellation be incomplete, and it affects the system performance of proposed method. Our novel method is compared with the NOMA and beamforming methods based on several terms, such as the number of users, channel gain, and accuracy of channel matrix estimation. In the case of poor channel gain and low transmit power, the channel capacity of proposed method is slightly lower than that of 2 other methods. However, the proposed method outperforms in other considered scenarios. Our proposed method can provide a

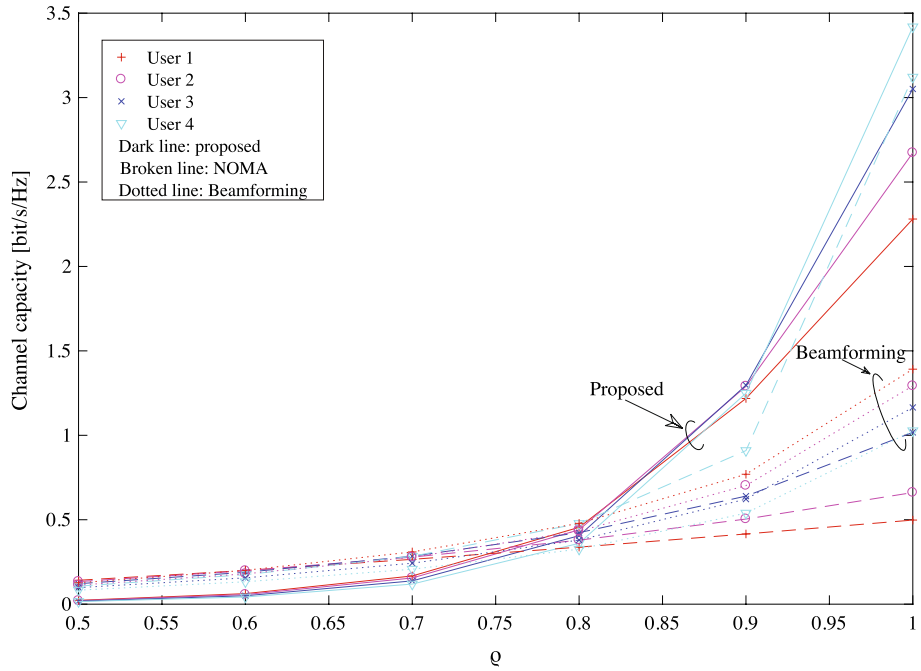

Fig. 8 The channel capacity via ρ with $\delta = 15$ dB and $\gamma = 0.2$

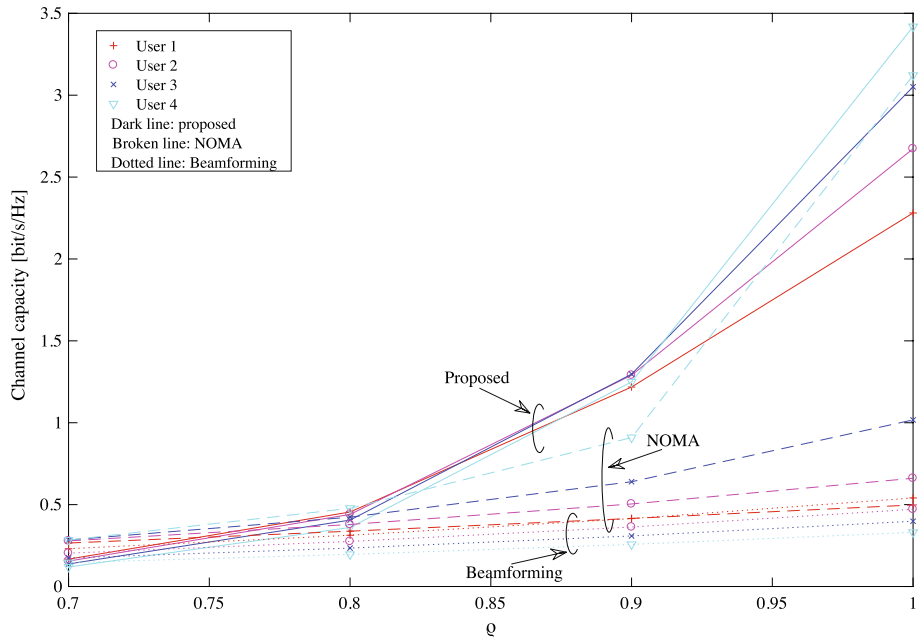

Fig. 9 The channel capacity via ρ with $\delta = 15$ dB and $\gamma = 0.9$

high quality of service for multiple users systems with few antennas. Therefore, it can be applied to advanced MU-MIMO systems to improve the channel capacity, especially for the system with compact base station, few antennas and serving many users.

In our future works, the proposed method will be discussed on other criteria, such as complexity, bit error rate and so on. Furthermore, the number of antennas at users was fixed to 2 for accommodating personal devices in MU-MIMO systems. The proposed method will be considered to apply to another system with different scenario, e.g., variable number of antennas at users.

Abbreviations

BS: Base station; MU: Multiple users; MIMO: Multiple input multiple output; NOMA: Non-orthogonal multiple access; SIC: Successive interference cancellation; SINR: Signal-to-interference-plus-noise ratio; SNR: signal-to-noise ratio; ZFBF: Zero forcing beamforming.

Acknowledgements

Not applicable.

Author contributions

The contribution of Nguyen Thu Phuong contains methodology, investigation, and writing–review and editing. The contribution of Vu Van Son is investigation, formal analysis, and writing–original draft preparation. The contribution of Pham Thanh Hiep is conceptualization, formal analysis, and writing–original draft preparation.

Funding

This research is funded by Vietnam National Foundation for Science and Technology Development (NAFOSTED) under grant number 102.04-2017.311

Availability of data and materials

Data used to support the findings of this study are already available in the manuscript.

Declarations

Consent for publication

All authors have agree and given their consent for submission of this paper to EURASIP Journal on Wireless Communications and Networking.

Competing interests
The authors declare that they have no competing interests.

Received: 21 December 2021 Accepted: 29 March 2022
Published online: 08 April 2022

References

1. L. Claudino, T. Abrao, Efficient ZF-WF strategy for sum-rate maximization of MU-MISO cognitive radio networks. AEU Int. J. Electron. Commun. **84**, 366–374 (2018)
2. G.-W. Jung, H.-K. Kim, Y.-H. Lee, Zero-forcing beamforming with user grouping in spatially correlated channel environments, in *International Conference on Computing, Networking and Communications (ICNC)* (2020)
3. H.A. Ammar, R. Adve, S. Shahbazpanahi, G. Boudreau, Statistical analysis of downlink zero-forcing beamforming. IEEE Wirel. Commun. Lett. **9**(11), 1965–1969 (2020)
4. S. Mondal, J. Paramesh, A reconfigurable 28-/37-GHz MMSE-adaptive hybrid-beamforming receiver for carrier aggregation and multi-standard MIMO communication. IEEE J. Solid-State Circuits **54**(5), 1391–1406 (2019)
5. H.C. Mora, N.O. Garzon, C. de Almeida, Performance analysis of MC-CDMA cellular systems employing MMSE multiuser detector in presence of own-cell and co-cell interference. AEU Int. J. Electron. Commun. **80**, 19–28 (2017)
6. Q. Yu, C. Han, L. Bai, J. Choi, X. Shen, Low-complexity multiuser detection in millimeter-wave systems based on opportunistic hybrid beamforming. IEEE Trans. Veh. Technol. **67**(10), 10129–10133 (2018)
7. Y. Lin, S. Jin, M. Matthaiou, X. You, Transceiver design with UCD-based hybrid beamforming for millimeter wave massive MIMO. IEEE Trans. Commun. **67**(6), 4047–4061 (2019)
8. D. Zhang, J. Jiang, Hybrid dirty paper coding for massive multiuser MIMO system, in *IEEE International Conference on Signal Processing, Communications and Computing (ICSPCC)* (2017)
9. K. Ying, Z. Gao, S. Lyu, W. Yongpeng, H. Wang, M.-S. Alouini, GMD-based hybrid beamforming for large reconfigurable intelligent surface assisted millimeter-wave massive MIMO. IEEE Access **8**, 19530–19539 (2020)
10. T. Peken, S. Adiga, R. Tandon, T. Bose, Deep learning for SVD and hybrid beamforming. IEEE Trans. Wirel. Commun. **19**(10), 6621–6642 (2020)
11. G.M. Zilli, W.-P. Zhu, Constrained-SVD based hybrid beamforming design for millimeter-wave communications, in *IEEE 92nd Vehicular Technology Conference (VTC2020-Fall)* (2020)
12. H.J. Kwon, J.H. Lee, W. Choi, Machine learning-based beamforming in two-user MISO interference channels, in *International Conference on Artificial Intelligence in Information and Communication (ICAIIC)* (2019)
13. X. Zhou, Y. Li, W. Liang, CNN-RNN based intelligent recommendation for online medical pre-diagnosis support. IEEE/ACM Trans. Comput. Biol. Bioinform. **18**(3), 912–921 (2021). https://doi.org/10.1109/TCBB.2020.2994780
14. X. Zhou, W. Liang, K.I.-K. Wang, L.T. Yang, Deep correlation mining based on hierarchical hybrid networks for heterogeneous big data recommendations. IEEE Trans. Comput. Soc. Syst. **8**(1), 171–178 (2021). https://doi.org/10.1109/TCSS.2020.2987846
15. S. Katla, L. Xiang, Y. Zhang, M. El-Hajjar, A.A.M. Mourad, L. Hanzo, Deep learning assisted detection for index modulation aided mmWave systems. IEEE Access **8**, 202738–202754 (2020)
16. H. Xie, B. Wang, F. Gao, S. Jin, A full-space spectrum-sharing strategy for massive MIMO cognitive radio. IEEE J. Sel. Areas Commun. **34**(10), 2537–2549 (2016)
17. H. Xie, F. Gao, S. Zhang, S. Jin, A unified transmission strategy for TDD/FDD massive MIMO systems with spatial basis expansion model. IEEE Trans. Veh. Technol. **66**(4), 3170–3184 (2017)
18. M.S. Aljumaily, Hybrid beamforming in massive-MIMO mmWave systems using LU decomposition, in *IEEE 90th Vehicular Technology Conference (VTC2019-Fall)* (2019)
19. N.T. Nguyen, K. Lee, Unequally sub-connected architecture for hybrid beamforming in massive MIMO systems. IEEE Trans. Wirel. Commun. **19**(2), 1127–1140 (2020)
20. B. Wang, F. Gao, S. Jin, H. Lin, G.Y. Li, Spatial- and frequency-wideband effects in millimeter-wave massive MIMO systems. IEEE Trans. Signal Process. **66**(13), 3393–3406 (2018)
21. S. Jayaprakasam, X. Ma, J.W. Choi, S. Kim, Robust beam-tracking for mmWave mobile communications. IEEE Commun. Lett. **21**(12), 2654–2657 (2017)
22. T.M. Hoang, V.V. Son, N.C. Dinh, P.T. Hiep, Optimizing duration of energy harvesting for downlink NOMA full-duplex over Nakagami-m fading channel. Int. J. Electron. Commun. (AEU) **95**, 199–206 (2018)
23. T.C. Hieu, N.L. Cuong, T.M. Hoang, D.T. Quan, P.T. Hiep, On outage probability and ergodic rate of downlink multi-user relay systems with combination of NOMA, SWIPT, and beamforming. Sensors **20**, 4737 (2020). https://doi.org/10.3390/s20174737
24. H.D. Vinh, V.V. Son, T.M. Hoang, P.T. Hiep, *Proposal of combination of NOMA and beamforming methods for downlink multi-users systems, in The 3rd International Conference on Recent Advances in Signal Processing, Telecommunications & Computing (SigTelCom)* (Vietnam, Ha noi, 2019), pp. 20–24
25. S. Chinnadurai, P. Selvaprabhu, Y. Jeong, A.L. Sarker, H. Hai, W. Duan, M.H. Lee, User clustering and robust beamforming design in multicell MIMO-NOMA system for 5G communications. AEU Int. J. Electron. Commun. **78**, 181–191 (2017)
26. P.T. Hiep, R. Kohno, Water-filling for full-duplex multiple-hop MIMO relay system. EURASIP J. Wirel. Commun. Netw. **2014**, 174 (2014)
27. B.Q. Doanh, T.C. Hieu, T.S. Nam, P.T.P. Anh, P.T. Hiep, Performance analysis of joint precoding and equalization design with shared redundancy for imperfect CSI MIMO systems. Adv. Sci. Technol. Eng. Syst. J. **5**(3), 142–149 (2020)
28. P.T. Hiep, T.M. Hoang, Non-orthogonal multiple access and beamforming for relay network with RF energy harvesting. ICT Express **6**, 11–15 (2020)

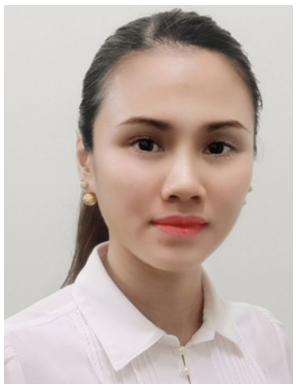

Nguyen Thu Phuong received the B.S, M.S and Ph.D. degrees from Le Quy Don Technical University, Vietnam, in 2008, 2012 and 2016, respectively. She is now a lecturer at Faculty of Radio-Electronics Engineering, and a key member of Advanced Wireless Communication Group, Le Quy Don Technical University, Hanoi, Vietnam. Her research interests are in the area of emerging technologies for future wireless communications: spatial modulation and index modulation, non-orthogonal multiple access (NOMA), space-time processing, space-time coding and MIMO systems.

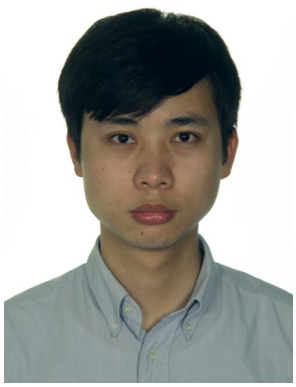

Vu Van Son received the B.E. degree from the Le Quy Don Technical University, in 2004; received the Ph.D. degree in Radio-physics, Electronic and Medicine Engineering from the Vladimir State University, Russia, in 2009. His previous research interests have included stochastic processes, wireless communications, pattern recognition, and neural networks. His current work is mainly focused on wireless communications, with special emphasis on modeling, estimation, and efficient simulation of wireless channels, and system performance analysis.

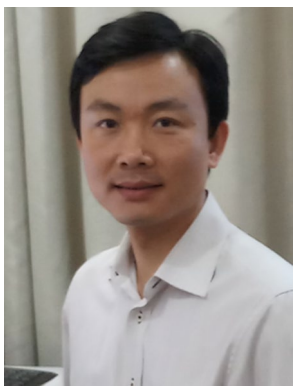

Pham Thanh Hiep received the B.E. degree in Communications Engineering from National Defense Academy, Japan, in 2005; received the M.E. and Ph.D. degree in Physics, Electrical and Computer Engineering from Yokohama National University, Japan, in 2009 and 2012, respectively. He was working as associate researcher at Yokohama National University, Yokohama, Japan, from 2012 to 2015. Now, he is a lecturer at Le Quy Don Technical University, Ha Noi, Viet Nam. His research interests lie in the area of wireless information and communications technologies.